Quantum oscillations between close-lying states mediated by the electronic continuum in intense high-frequency pulses

Philipp V. Demekhin and Lorenz S. Cederbaum

Phys. Rev. A **91**, 013417 — Published 28 January 2015

DOI: 10.1103/PhysRevA.91.013417

Quantum oscillations between close-by states mediated by the electronic continuum in intense high-frequency pulses

Philipp V. Demekhin[1,*] and Lorenz S. Cederbaum[2]

[1]*Institut für Physik, Universität Kassel,*

Heinrich-Plett-Strasse 40, D-34132 Kassel, Germany

[2]*Theoretische Chemie, Physikalisch-Chemisches Institut, Universität Heidelberg,*

Im Neuenheimer Feld 229, D-69120 Heidelberg, Germany

Abstract

The dynamics of neighboring states exposed to short intense laser pulses of carrier frequencies well above the ionization threshold of the system is investigated theoretically in the dipole approximation. It is shown that the ionizing pulse induces a time-dependent non-hermitian coupling between these states determined by the Raman-coupling and the direct ionization probability. This coupling induces quantum oscillations between the neighboring states while the strong pulse is on. The phenomenon opens the possibility to achieve a coherent control over the populations of neighboring states by short intense ionizing pulses. The present numerical results suggest exciting applications for FEL and attosecond experiments.

PACS numbers: 33.20.Xx, 41.60.Cr, 82.50.Kx

INTRODUCTION

Nearly-resonant optical transitions between two bound electronic states of a system mediated by intense laser pulses are accompanied by Rabi oscillations. This phenomenon is a basic example of coherent nonlinear light-matter interaction; it is fundamental to quantum physics and has no classical analog [1, 2]. Initiating Rabi cycles between different levels of a three-level system is routinely used in the stimulated Raman adiabatic passage (STIRAP) technique [3] to efficiently accomplish population transfer between two states which are coupled via an intermediate bound state by a counter intuitive sequence of *two nearly resonant* partly overlapping optical pulses. An intense laser pulse can also couple a bound state with the continuum to create the so-called laser-induced continuum structure (LICS) [4]. This structure can be probed by a second laser field which ionizes another bound state into the continuum state of the same energy and symmetry as LICS. If the probe pulse is relatively weak, the situation becomes analogous to that of Fano interference [5] with tunable energy position and width of the resonant state in the LICS. If both laser pulses are strong, the two bound states become coupled to each other through the common LICS via the Raman transition [4]. This situation resembles (impulsive) stimulated Raman scattering [6, 7] via a continuum state. It was first demonstrated theoretically [8, 9] that continuum state can serve as an intermediate state to transfer population between two discrete states by means of STIRAP. This transfer is, however, incomplete [10] in comparison with the situation encountered with a discrete intermediate state [3]. STIRAP schemes utilizing intermediate continuum [11] have been successfully implemented in several atomic and molecular [12–18] systems.

The new generation of light sources, like free electron lasers [19–21] and high-order harmonic generation setups [22, 23], offers the possibility to explore the strong-field and short-pulse limits of coherent nonlinear light-matter interactions in the high-frequency regime. For selected theoretical and experimental studies see, e.g., Refs. [24–35] and references therein. In the high-frequency regime, already a single high-energy photon allows one to directly access the electron spectrum of a system deep in the continuum, and to selectively trigger or probe the segregated dynamics of well-separated highly-excited transient states. In addition to the appearance of new phenomena, many basic phenomena known from the optical regime may also persist in the high-frequency regime. For instance, damped Rabi oscillations spec-

tacularly modify the Auger decay processes in atoms [36–40] and molecules [41–43] exposed to strong nearly-resonant high-frequency pulses.

In the present work we illustrate how the Raman-coupling between discrete states via a common continuum can be exploited in the high-frequency regime. To be specific, we derive the equations describing the interaction of two energy levels with a single short high-frequency pulse and analyze the information contained in this model. We shall demonstrate here that the pulse-induced coupling between the two states, resulting in quantum oscillations between them, can significantly modify dynamics of the photoionization process. The phenomenon of population transfer happens here already with a *single pulse*, i.e., under different conditions than in STIRAP schemes utilizing intermediate continuum [11]. Actually, it typically happens when matter is exposed to, e.g., free electron lasers, and can be exploited to manipulate the coherent dynamics of a system driven by a single intense ionizing pulse. The energy levels can be, for instance, fine-structure electronic sub-levels of an atom, nuclear vibrational states of a molecule, or, depending on the pulse duration and intensity, any bound states which couple to the same continuum. The present results and the conclusions drawn are general and can straightforwardly be extended to more energy levels coupled by a single ionizing pulse.

THEORY

Consider a system of two electronic states $|I_1\rangle$ and $|I_2\rangle$ with energies E_1 and E_2 and initial population amplitudes a_1^0 and a_2^0 at time $t = 0$. A linearly polarized probe pulse $\mathcal{E}(t)$ of sufficiently large carrier frequency ω ionizes this system by bringing it to the continuum state $|F\varepsilon\rangle$ of the ion of energy E_F and photoelectron of kinetic energy ε well above the ionization threshold. The total time-dependent wave function of the system reads [37, 44, 45]:

$$\Psi(t) = a_1(t)|I_1\rangle + a_2(t)|I_2\rangle + \int d\varepsilon\, a_\varepsilon(t)|F\varepsilon\rangle, \tag{1}$$

where $a_1(t)$, $a_2(t)$, and $a_\varepsilon(t)$ are the time-dependent amplitudes of the populations of the corresponding electronic states. Substituting $\Psi(t)$ into the time-dependent Schrödinger equation for the system and implying the dipole approximation for its interaction with the laser field, we obtain the following set of time-evolution equations for these amplitudes (atomic

units are used throughout)

$$i\dot{a}_1(t) = E_1 a_1(t) + \int d\varepsilon\, d^\dagger_{1\varepsilon} \mathcal{E}(t)\, a_\varepsilon(t), \tag{2a}$$

$$i\dot{a}_2(t) = E_2 a_2(t) + \int d\varepsilon\, d^\dagger_{2\varepsilon} \mathcal{E}(t)\, a_\varepsilon(t), \tag{2b}$$

$$i\dot{a}_\varepsilon(t) = \left[d_{1\varepsilon} a_1(t) + d_{2\varepsilon} a_2(t)\right] \mathcal{E}(t) + (E_F + \varepsilon)\, a_\varepsilon(t), \tag{2c}$$

where $d_{j\varepsilon} = \langle F\varepsilon|\hat{z}|I_j\rangle$ are the corresponding energy dependent ionization dipole transition matrix elements.

The above equations contain much physics, but are difficult to solve and to analyze. One can decouple the first two from the last equation and at the same time simplify the complicated integrals appearing there by employing the local approximation [46, 47]. This approximation eliminates the temporal memory effects due to the nonlocality of the formal solution of Eq. (2c) in time [44]. To be specific, we consider pulses $\mathcal{E}(t) = \mathcal{E}_0\, g(t) \cos\omega t$ with a single carrier high frequency and a pulse envelope $g(t)$ which varies slowly compared to the duration of a cycle. In the local approximation, Eqs. (2a) and (2b) simplify to the following compact form $(j, k = 1, 2)$:

$$i\dot{a}_j(t) = E_j\, a_j(t) + \sum_k \left(\Delta_{jk} - \frac{i}{2}\Gamma_{jk}\right) g^2(t)\, a_k(t). \tag{3}$$

The derivation of Eqs. (3) is analogous to that in the appendices of Refs. [37, 45].

In Eqs. (3), the terms Δ_{jk} arise due to the ac Stark effect [48] induced by the intense probe pulse. The explicit expression for Δ_{jk} reads

$$\Delta_{jk} = -\mathcal{P} \int \frac{d^\dagger_{j\varepsilon} d_{k\varepsilon} \mathcal{E}_0^2}{4} \left(\frac{d\varepsilon}{E_{Fk} + \varepsilon - \omega} + \frac{d\varepsilon}{E_{Fk} + \varepsilon + \omega}\right), \tag{4}$$

where $\mathcal{P}$ denotes the principal value of the integral and $E_{Fk} = E_F - E_k$ stands for the ionization potentials of the two levels. The diagonal shifts $\Delta_{jj} g^2(t)$ are the temporal ac Stark energy-shifts due to the interaction of the initial electronic state $|I_j\rangle$ with the electronic continuum $|F\varepsilon\rangle$, for which Eq. (4) coincides with the previously derived expression for Δ [45, 49]. Analogously, we obtain

$$\Gamma_{jk} = 2\pi\, \frac{d^\dagger_{j\varepsilon_0} d_{k\varepsilon_0} \mathcal{E}_0^2}{4}\,, \tag{5}$$

where $d_{k\varepsilon_0}$ is the value of the matrix element at the pole $\varepsilon_0 = \omega - E_{Fk}$ in Eq. (4). The diagonal terms $\Gamma_{jj} g^2(t)$ are the temporal total photoionization rates of the initial states and

describe the losses of the corresponding populations due to the ionization [37, 45, 49]. As usual [48], all the shifts and rates are proportional to the peak intensity $I_0 \propto \mathcal{E}_0^2$, and their contributions follow the pulse intensity envelope $g^2(t)$. In the case of several continua, one has simply to sum over all possible individual shifts Δ_{jk} (4) and rates Γ_{jk} (5) of only open ionization channels on the right-hand side of Eq. (3).

Apart from the diagonal quantities discussed above, Eqs. (3) contains non-diagonal elements Δ_{jk} and Γ_{jk} with $j \neq k$, which couple the two states. To further illuminate the physics at hand, let us analyze the impact of these non-diagonal corrections on the coherent dynamics of the system and provide them with physical interpretation. We first notice that the dynamics of the initial energy levels in the local approximation is completely decoupled from the time-evolution of the final continuum states. The latter follows from Eq. (2c) once the dynamics of the initial levels has been determined. Eqs. (3) can be viewed as a time-dependent matrix Schrödinger equation for the amplitudes where the dynamics is governed by the following 2×2 effective Hamiltonian

$$\mathbf{H}(t) = \begin{bmatrix} E_1 + \left(\Delta_{11} - \frac{i}{2}\Gamma_{11}\right) g^2(t) & \left(\Delta_{12} - \frac{i}{2}\Gamma_{12}\right) g^2(t) \\ \left(\Delta_{21} - \frac{i}{2}\Gamma_{21}\right) g^2(t) & E_2 + \left(\Delta_{22} - \frac{i}{2}\Gamma_{22}\right) g^2(t) \end{bmatrix}. \tag{6}$$

Although we consider here a very different scenario with a single ionizing high-frequency pulse, we would like to mention that the presently derived Hamiltonian (6) is closely related to that describing STIRAP schemes utilizing intermediate continuum (see, e.g., Refs. [10, 11]).

According to (6), the energies $E_{j=1,2}$ of the initial states experience time-dependent ac Stark shifts $\Delta_{jj} g^2(t)$ and their populations leak by the time dependent ionization rates $\Gamma_{jj} g^2(t)$ into all final continuum states. Importantly, the two initial states do couple to each other by the non-hermitian time-dependent coupling $\left(\Delta_{jk} - \frac{i}{2}\Gamma_{jk}\right) g^2(t)$, $j \neq k$, induced by the high-frequency pulse. This coupling is indirect and mediated via the ionization continuum, and can be interpreted as follows: The photoelectron emitted by one of the initial states, say $|I_1\rangle$, is recaptured by the residual ion to produce the other initial state, $|I_2\rangle$, and vice versa (see also below). This coupling is also known as the Raman-coupling [4]. One may expect that this coupling, as any other coupling, induces quantum oscillations between the states, and this provides direct coherent control over the populations of these states.

One can first compute the dynamics of the initial states via the Hamiltonian (6) and subsequently use this dynamics to determine the amplitudes of the continuum states via Eq. (2c) and with it the measurable photoelectron spectrum as

$$\sigma(\varepsilon) = |a_\varepsilon(+\infty)|^2. \tag{7}$$

Intuitively the initial states loose populations due to ionization by the laser pulse and these are transferred to the continuum. A fundamental question immediately arises: Can populations be transferred back to the initial states in spite of the high frequency and the single pulse used? The answer is yes, and we shall also see it clearly in the model numerical applications below. Obviously, this is only possible by the Raman-coupling $\left(\Delta_{jk} - \frac{i}{2}\Gamma_{jk}\right) g^2(t)$ with $j \neq k$ induced by the laser pulse. Importantly, this can also be seen in the norm of the total wave function (1) which should be equal to 1 at all times, and is not so if we neglect the above coupling. One can show that all elements $\left(\Delta_{jk} - \frac{i}{2}\Gamma_{jk}\right) g^2(t)$ together are responsible for the conservation of the norm as a function of time:

$$|\Psi(t)|^2 = |a_1(t)|^2 + |a_2(t)|^2 + \int d\varepsilon |a_\varepsilon(t)|^2 = 1. \tag{8}$$

This result illustrates the relevance of the states' coupling for the theoretical description of systems exposed to high-frequency pulses.

RESULTS AND DISCUSSION

We illustrate the impact of the coupling of two nearby states via the continuum by studying an explicit model numerical example with judiciously chosen parameters. One can always set the energy of the first state to be the origin of the energy scale ($E_1 = 0$). We choose $E_2 = 0.2$ eV and the pulse ionizing these two states to be Gaussian-shaped $g(t) = exp(-(t - \Delta t)^2/\tau^2)$ with a duration $\tau = 10$ fs and a carrier frequency $\omega = 39.9$ eV which takes both states into the continuum well above the energy of the ionic state $E_F = 10$ eV. The ionization dipole transition matrix elements $d_{j\varepsilon}$ are both taken to be equal to 0.1 a.u., which is comparable with the value of 0.092 a.u. computed for the H 1s-state at the chosen ω. The impact is studied for pulse intensities in the range from 10^{13} to 10^{15} W/cm^2 for which the ionization rates Γ_{jk} computed via Eq. (5) are between 0.12 meV and 12 meV. Finally, to calculate the Δ_{jk} which provide the ac Stark shifts is a formidable task [48].

In Eq. (4) one sees that one has to know the energy dependence of the transition matrix elements. Depending on the field intensity and carrier frequency the ac Stark shifts can be sizable, up to a few eV [45, 49]. In our example, the shifts Δ_{jk} are free parameters, and they all are taken to be equal and to be between 0.002 and 0.2 eV in the range of intensities given above (note that due to Eq. (4) these shifts scale linearly with the intensity). The judiciously chosen values of Δ_{jk} are comparable with the respective ponderomotive energies $U_p = \mathcal{E}_0^2/4\omega^2$ [50] for the present parameters.

In the first application we assume that only one of the two electronic states $|I_j\rangle$ is initially populated, and study both cases where either state 1 or state 2 is the populated state. Fig. 1 summarizes the results. In the upper panel it is seen that the final populations $|a_j|^2$ after the ionizing pulse has expired exhibit clear oscillations as a function of the field intensity. Moreover, in both cases the initially non-populated level acquires substantial population. This is due to the population transfer governed by the pulse-induced non-hermitian coupling between the states in Eq. (6). In spite of the fact that the photon energy $\omega = 39.9$ eV is much larger than the energy splitting $E_2 - E_1 = 0.2$ eV, the pulse induces quantum oscillations. Without the coupling, the initially unpopulated state will stay unpopulated and the population of the other one will just decrease monotonously by ionization.

As a consequence of the found efficient population transfer, one can even expect photoelectrons to come from the ionization of the initially unpopulated state. The photoelectron spectra computed for the peak intensity of 10^{15} W/cm^2 using Eq. (7) are depicted in the lower panel of Fig. 1. Indeed, the spectra show clear peaks associated with the ionization of the initially unpopulated level. They differ substantially from the weak field spectra which would exhibit a single peak at the positions indicated in the panel. Moreover, even the energies of the first peak in the spectra differ considerably from each other depending on which level is initially unpopulated.

In the second application, we assume that a pump pulse creates at time $t = 0$ a coherent superposition of the neighboring states. Because of different time-evolutions of the individual states, complicated dynamics of the coherently created wave packet may begin. For instance, the coherent population of electronic levels of an ion may cause charge migration in molecules [51–53], or in the case of vibrational molecular states, nuclear wave packet dynamics is initiates [54–56]. Then, after a free evolution in time and space, this wave packet is probed by an ionizing high-frequency pulse. Because of temporal coherence of the driving pulse,

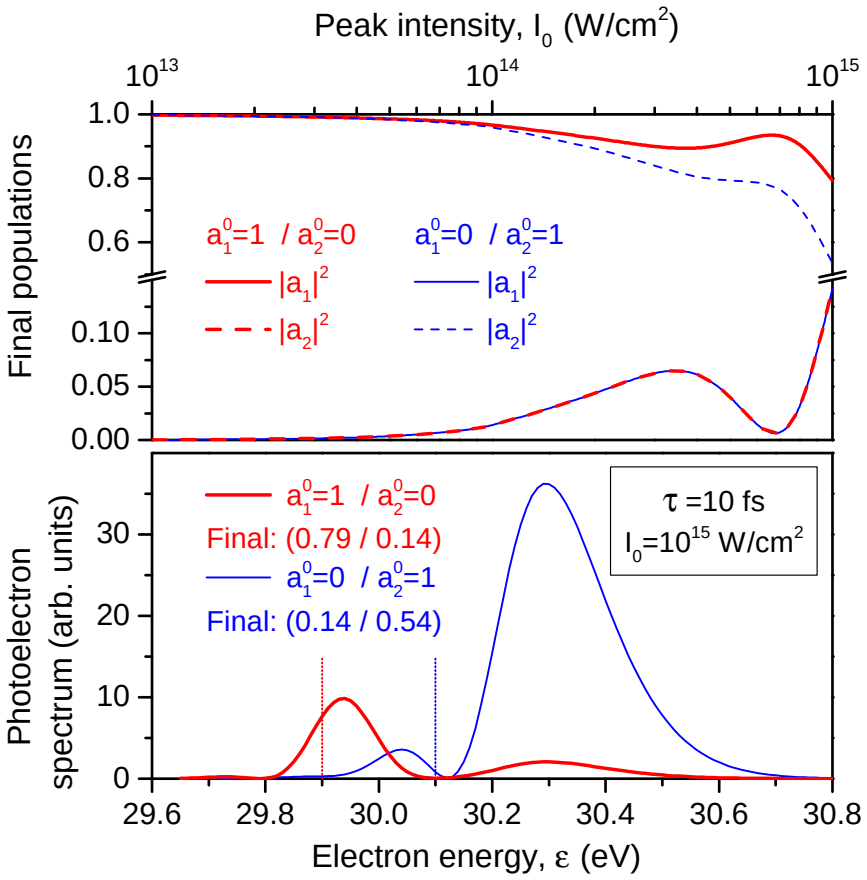

FIG. 1: (Color online) Results for the model of two neighboring electronic states of which one is initially unpopulated. The system is exposed to a high-frequency ionizing laser pulse (see text for details). *Upper panel:* residual populations of the states after the ionizing pulse has expired as a function of the peak intensity of the pulse. Population transfer between the states and quantum oscillations are clearly seen. *Lower panel:* photoelectron spectra for the peak intensity 10^{15} W/cm^2. Due to the population transfer dictated by the non-hermitian coupling between the states in Eq. (6), each spectrum exhibits two peaks instead of only one expected in a weak field at either 29.9 or 30.1 eV as indicated by vertical lines.

interesting interference effects emerge in the resulting probe-pulse-spectra [54–60]. These effects are associated with the phase accumulated by the free system during the time delay between the two pulses [61].

In the numerical calculations we use the same parameters as above and assume that the pump pulse has populated the two states at $t = 0$ with equal real amplitudes $a_1^0 = a_2^0 = 1/\sqrt{2}$. The coherent wave packet starts to evolve periodically in time with the period given by the

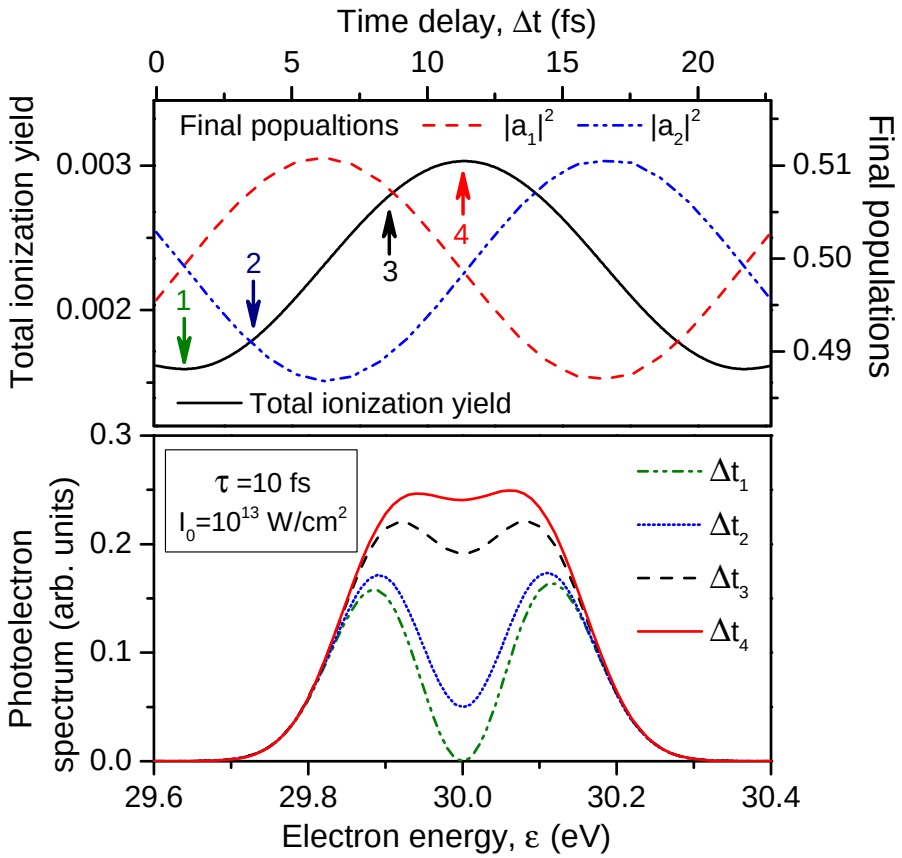

FIG. 2: (Color online) Results for the model of two neighboring electronic states where both are initially coherently populated, for example, by a pump pulse (conditions at $t = 0$: $a_1^0 = a_2^0 = 1/\sqrt{2}$). After a time delay of Δt the system is exposed to a weak high-frequency ionizing probe pulse (see text for details). *Upper panel:* the total ionization yield (solid curve) and residual populations of the states after the probe pulse has expired (broken curves) as a function of the time-delay between the pump and probe pulses. *Lower panel:* photoelectron spectra computed for those time-delays Δt which are indicated in the upper panel by vertical arrows.

energy splitting: $T = 2\pi/(E_2 - E_1) \approx 20.7$ fs. A probe pulse ionizes this system after a time-delay Δt which is large enough to avoid the overlap of the pump and probe pulses. Δt and the phase difference between the populations $a_j(t)$ are, of course, intimately related, and, thus, choosing different phases for the initial conditions a_j^0 simply reduces to a change of Δt.

We first consider a relatively weak probe pulse of 10^{13} W/cm^2 peak intensity. The results are summarized in Fig. 2. As seen in the upper panel, the total ionization yield of the system (solid curve) possesses oscillations as a function of the time-delay Δt. The phenomenon is

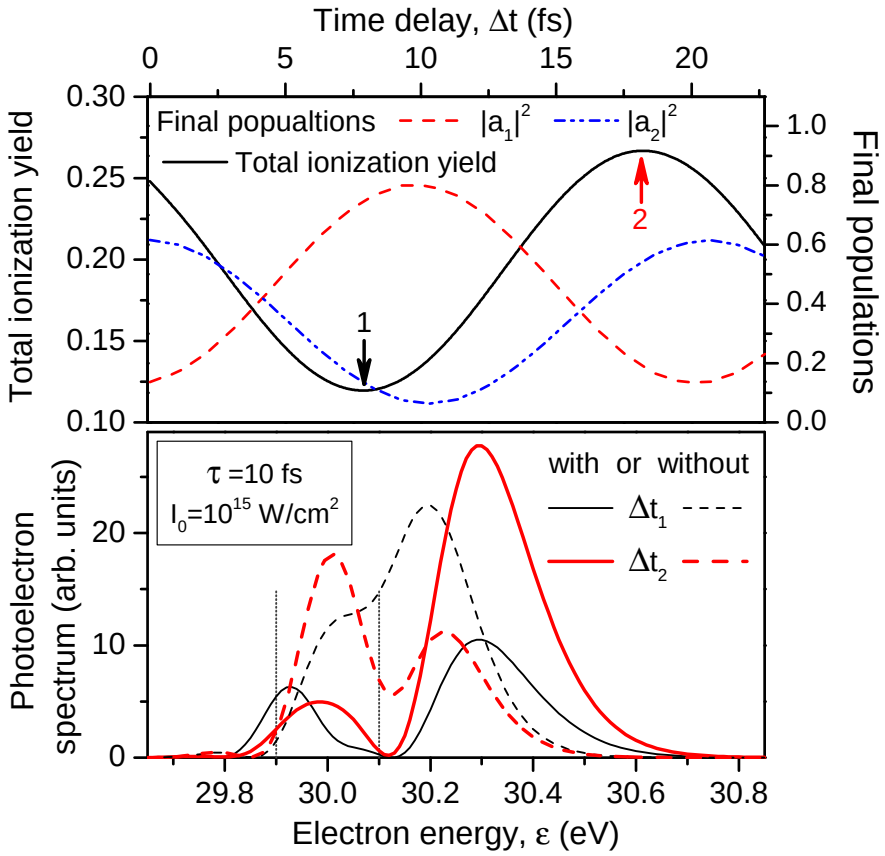

FIG. 3: (Color online) As in Fig. 2 except that the probe pulse is now more intense (peak intensity 10^{15} instead of 10^{13} W/cm^2). In addition to Fig. 2, the spectra computed by neglecting the pulse-induced coupling between the states are also shown for comparison in the lower panel (dashed curves).

already known [56–58, 61], and is the result of the interference of the photoelectrons emitted from the two neighboring initially populated states. This can be seen from the spectra computed for different Δt shown in the lower panel which are indeed very different. What is a new phenomenon here is that owing to the pulse-induced couplings the populations of the two states after the probe pulse has expired also exhibit oscillations with Δt (broken curves in the upper panel). Without these coupling the residual populations $|a_j|^2$ would be independent of the time delay Δt. It is gratifying to note that even for the relatively weak pulse, the final populations can be slightly larger than their initial values of $\frac{1}{2}$ due to the population transfer mentioned above.

What happens if the system is probed by an intense pulse? Here, according to Eq. (4), the coupling which was chosen $\Delta_{jk} = 0.002$ eV for 10^{13} W/cm^2 is now $\Delta_{jk} = 0.2$ eV for

10^{15} W/cm^2 peak intensity and comparable to the energy splitting $E_2 - E_1 = 0.2$ eV, making the changes caused by the probe pulse dramatic. Fig. 3 summarizes our results for a peak intensity of 10^{15} W/cm^2. One can see that the variations in the ionization yield with Δt (solid curve in the upper panel) are now substantial and range from 0.12 to 0.27, a magnitude which is easier to distinguish experimentally. The residual populations of the initial states (broken curves in the upper panel) can now vary enormously and even arrive at 0.8. Obviously, in spite of the strong ionization in the intense field, the non-hermitian couplings manage to transfer significant population between the states, so that a final population can become much larger than the initial population of $|a_j^0|^2 = \frac{1}{2}$. This gives room for manipulating populations of nearby levels by high-frequency ionizing pulses.

The photoelectron spectra are also very different from the weak-field ones (cf., lower panels of Fig. 2 and 3). They are substantially shifted from the weak field positions and each of the two peaks possesses a very strong asymmetry and their relative intensities are strongly asymmetric too. The lower panel of Fig. 3 illustrates that the pulse-induced coupling plays an important role in the formation of the photoionization spectrum. Indeed, the spectra computed by neglecting the coupling $\left(\Delta_{jk} - \frac{i}{2}\Gamma_{jk}\right) g^2(t)$, $j \neq k$, (but not the ionization losses Γ_{jj} and ac Stark shifts Δ_{jj}, $j = 1, 2$ on the diagonal of Eq. (6)) shown as dashed curves look very different from the 'true' spectra depicted as solid curves.

CONCLUSIONS

Let us briefly conclude. Photoionization of coherently superimposed states is usually accompanied by interesting interference effects which are prominently manifested in the observable quantities. Here we show that the Raman-coupling induced by an intense high-frequency ionizing pulse between two neighboring states via a common continuum can cause substantial population transfer between these states even if only one of them was initially populated, modify thereby the coherent dynamics of the system, and significantly influence the photoionization process. In the case of several neighboring states, a single high-frequency pulse can simultaneously couple all the states participating in the ionization. The coupling is mediated by the continuum and is a complex quantity which grows linearly with the intensity of the pulse. Increasing this intensity within a realistic range can make the influence of the coupling sizable. This should be clearly observable in the photoelectron spectrum,

total ionization yield, and residual populations of the initially populated states and their neighboring states. The present results are general and expected to be of particular relevance to femtosecond and attosecond spectroscopy.

We have discussed the impact of the high-frequency pulse both as a pump and a probe pulse and believe that the discussed effects can be verified experimentally by currently available sources of intense high-frequency pulses. For instance, the free electron laser FLASH [19] generates soft x-ray radiation in the energy range of 26–180 eV with flux of about 10^{13} photons per pulse with durations of 10–70 fs [62], and it can yield the peak intensity of more than 10^{16} W/cm^2 [63]. In addition, the free electron laser facility FERMI at Elettra [64] operates in single-mode, providing coherent pulses with durations of 30 to 100 fs in the photon energy range of 12 to 413 eV, and it is expected to provide a flux of about 10^{14} photons per pulse. Alternatively, perfectly coherent and monochromatic pulses from high-order harmonic generation techniques [22, 23], with the duration down to 0.1 fs, carrier frequencies in the range from 30 to 110 eV, and peak intensities of up to 5×10^{14} W/cm^2, can also be utilized. Thus, the necessary pulse durations, photon energies, temporal coherence, and peak intensities are available at present. Our results refer to basic physics a single atom or molecule undergoes when exposed to a coherent and monochromatic high-frequency pulse. The knowledge of this physics is prerequisite to simulate real experiments.

T. Baumert, A. Senftleben, and S. Klaiman are gratefully acknowledged for many fruitful discussions. The work was partly supported by the State Hessen LOEWE program within the focus-project ELCH and by the Deutsche Forschungsgemeinschaft (DFG).

---

* Electronic address: demekhin@physik.uni-kassel.de

[1] L. Allen and J.H. Eberly, *Optical Resonance and Two-Level Atoms* (Dover, New York, 1975).

[2] P. Meystre and M. Sargent III, *Elements of Quantum Optics* (Springer, Berlin, 1991).

[3] K. Bergmann, H. Theuer, and B.W. Shore, Rev. Mod. Phys. **70**, 1003 (1998).

[4] P.L. Knight, M.A. Lauder, and B.J. Dalton, Phys. Rep. 190, 1 (1990).

[5] U. Fano, Phys. Rev. **124**, 1866 (1961).

[6] L. Dhar, J.A. Rogers, and K.A. Nelson, Chem. Rev. **94**, 157 (1994).

[7] *Raman Scattering in Materials Science*, (edited by W.H. Weber and R. Merlin), *Springer*

Series in Materials Science Vol. **42** (Springer, Berlin, 2000).

[8] C.E. Carroll and F.T. Hioe, Phys. Rev. Lett. **68**, 3523 (1992).

[9] C.E. Carroll and F.T. Hioe, Phys. Rev. A **47**, 571 (1993).

[10] T. Nakajima, M. Elk, J. Zhang, P. Lambropoulos, Phys. Rev. A **50**, R913 (1994).

[11] N.V. Vitanov and S. Stenholm, Phys. Rev. A **56**, 741 (1997).

[12] R.G. Unanyan, N.V. Vitanov, B.W. Shore, and K. Bergmann, Phys. Rev. A **61**, 043408 (2000).

[13] A.A. Rangelov, N.V. Vitanov, and E. Arimondo, Phys. Rev. A **76**, 043414 (2007).

[14] T. Peters, L.P. Yatsenko, and T. Halfmann, Phys. Rev. Lett. **95**, 103601 (2005).

[15] T. Peters and T. Halfmann, Opt. Commun. **271**, 475 (2007).

[16] P. Tran, Phys. Rev. A 59, 1444 (1999).

[17] Y.-C. Han, S.-M. Wang, K.-J. Yuan, S.-L. Cong, Chem. Phys. **333**, 119 (2007).

[18] T.-M. Yan, Y.-C. Han, K.-J. Yuan, S.-L. Cong, Chem. Phys. **348**, 39 (2008).

[19] W. Ackermann *et al.*, Nature Photon. **1** 336 (2007).

[20] P. Emma *et al.*, Nat. Photon. **4**, 641 (2010).

[21] L. Young *et al.*, Nature **466**, 56 (2010).

[22] G. Sansone *et al.*, Science **314** 443 (2006).

[23] E. Goulielmakis *et al.*, Science **320** 1614 (2008).

[24] Ph.V. Demekhin, S.D. Stoychev, A.I. Kuleff, and L.S. Cederbaum, Phys. Rev. Lett. **107**, 273002 (2011).

[25] N. Rohringer and R. Santra, Phys. Rev. A **86**, 043434 (2012).

[26] C. Buth *et al.*, J Chem. Phys. **136**, 214310 (2012).

[27] S.M. Cavaletto, C. Buth, Z. Harman, E.P. Kanter, S.H. Southwort, L. Young, and C.H. Keitel, Phys. Rev. A **86**, 033402 (2012).

[28] B. Rudek *et al.*, Nature Photonics, **6** 858 (2012).

[29] B. Rudek *et al.*, Phys. Rev. A **87**, 023413 (2013).

[30] K. Motomura *et al.*, J. Phys. B **46**, 164024 (2013).

[31] Ph.V. Demekhin, K. Gokhberg, G. Jabbari, S. Kopelke, A.I. Kuleff, and L.S. Cederbaum, J. Phys. B **46**, 021001 (2013).

[32] C. Weninger and N. Rohringer, Phys. Rev. A **88**, 053421 (2013).

[33] V. Kimberg and N. Rohringer, Phys. Rev. Lett. **110**, 043901 (2013).

[34] C. Weninger *et al.*, Phys. Rev. Lett. **111**, 233903 (2013).

[35] L.A.A. Nikolopoulos, Phys. Rev. Lett. **111**, 093001 (2013).

[36] N. Rohringer and R. Santra, Phys. Rev. A **77**, 053404 (2008).

[37] Ph.V. Demekhin and L.S. Cederbaum, Phys. Rev. A **83**, 023422 (2011).

[38] Ph.V. Demekhin and L.S. Cederbaum, Phys. Rev. A **86**, 063412 (2012).

[39] L.A.A. Nikolopoulos, T.J. Kelly, and J.T. Costello, Phys. Rev. A **84**, 063419 (2011).

[40] E.P. Kanter *et al.*, Phys. Rev. Lett. **107** 233001 (2011).

[41] L.S. Cederbaum, Y.-C. Chiang, Ph.V. Demekhin, and N. Moiseyev, Phys. Rev. Lett. **106**, 123001 (2011).

[42] Ph.V. Demekhin, Y.-C. Chiang, and L.S. Cederbaum, Phys. Rev. A **84**, 033417 (2011).

[43] Ph.V. Demekhin and L.S. Cederbaum, J. Phys. B **46**, 164008 (2013).

[44] Y.-C. Chiang, Ph.V. Demekhin, A.I. Kuleff *et al.*, Phys. Rev. A **81**, 032511 (2010).

[45] Ph.V. Demekhin and L.S. Cederbaum, Phys. Rev. A **88**, 043414 (2013).

[46] L.S. Cederbaum and W. Domcke, J. Phys. B **14**, 4665 (1981).

[47] W. Domcke, Phys. Rep. **208**, 97 (1991).

[48] B.J. Sussman, Am. J. Phys. **79**, 477 (2011).

[49] Ph.V. Demekhin and L.S. Cederbaum, Phys. Rev. Lett. **108**, 253001 (2012).

[50] M.V. Fedorov, *Atomic and Free Electrons in a Strong Light Field* (World Scientific, River Edge, 1997).

[51] L.S. Cederbaum and J. Zobeley, Chem. Phys. Lett. **307**, 205 (1999).

[52] A.I. Kuleff and L.S. Cederbaum, Phys. Rev. Lett. **98**, 083201 (2007).

[53] A.D. Dutoi, M. Wormit and L.S. Cederbaum, J. Chem. Phys. **134**, 024303 (2011).

[54] A. Assion, M. Geisler, J. Helbing *et al.*, Phys. Rev. A **54**, R4605 (1996).

[55] A. Assion, T. Baumert, M. Geisler *et al.*, Eur. Phys. J. D **4**, 145 (1998).

[56] M. Wollwnhaupt, V. Engel, and T. Baumert, Annu. Rev. Phys. Chem. **56**, 25 (2005).

[57] R.R. Jones, C.S. Raman, D.W. Schumacher, and P.H. Bucksbaum, Phys. Rev. Lett. **71**, 2575 (1993).

[58] Th. Ergler, B. Feuerstein, A. Rudenko *et al.*, Phys. Rev. Lett. **97**, 103004 (2006).

[59] A.T. Georges and P. Lambropoulos, Phys. Rev. A **18**, 1072 (1978).

[60] V. Schweigert and S. Mukamel, Phys. Rev. A **76**, 012504 (2007).

[61] V. Blanchet, C. Nicole, M.-A. Bouchene, and B. Girard, Phys. Rev. Lett. **78**, 2716 (1997).

[62] K. Tiedtke, *et al.*, New J. Phys. **11**, 023029 (2009).

[63] A.A. Sorokin, S.V. Bobashev, T. Feigl, K. Tiedtke, H. Wabnitz, and M. Richter, Phys. Rev. Lett. **99**, 213002 (2007).

[64] Home page of Free Electron Laser for Multidisciplinary Investigations FERMI at Elettra in Trieste, Italy, http://www.elettra.trieste.it/FERMI/